Anal. Chem. **2007,** *79,* 2483−2490

Analysis of Amino Acid Isotopomers Using FT-ICR MS

Francesco Pingitore,[†,‡] Yinjie Tang,[†,‡] Gary H. Kruppa,[§] and Jay D. Keasling*[,†,‡,∥]

Virtual Institute of Microbial Stress and Survival, Physical Biosciences Division, Lawrence Berkeley National Laboratory, Berkeley, California 94720, Bruker Daltonics Inc. Fremont, California 94538, and Departments of Chemical Engineering and Bioengineering, University of California, Berkeley, California 94720

Fluxes through known metabolic pathways and the presence of novel metabolic reactions are often determined by feeding isotopically labeled substrate to an organism and then determining the isotopomer distribution in amino acids in proteins. However, commonly used techniques to measure the isotopomer distributions require derivatization prior to analysis (gas chromatography/mass spectrometry (GC/MS)) or large sample sizes (nuclear magnetic resonance (NMR) spectroscopy). Here, we demonstrate the use of Fourier transform-ion cyclotron resonance mass spectrometry with direct infusion via electrospray ionization to rapidly measure the amino acid isotopomer distribution in a biomass hydrolysate of the soil bacterium *Desulfovibrio vulgaris* Hildenborough. By applying high front-end resolution for the precursor ion selection followed by sustained off-resonance irradiation collision-induced dissociation, it was possible to determine exactly and unambiguously the specific locations of the labeled atoms in the amino acids, which usually requires a combination of 2-D ^{13}C NMR spectroscopy and GC/MS. This method should be generally applicable to all biomass samples and will allow more accurate determination of metabolic fluxes with less work and less sample.

Quantification of fluxes through the central metabolism of organisms provides important information for annotating sequenced genomes, understanding how carbon is distributed through the various metabolic pathways in a cell, and rational optimization of metabolism in engineered microorganisms. Isotopomer profiling from ^{13}C tracer experiments is essential for metabolic flux analysis in complicated metabolic networks.[1,2] Very often, the targeted species for isotopomer analysis of metabolic fluxes are the amino acids. These species are synthesized from different precursors in central metabolism and, consequently, measuring their isotopomer distributions provides constraints for metabolic flux calculations in metabolic networks. Techniques like nuclear magnetic resonance (NMR) spectroscopy or gas chromatography coupled to mass spectrometric detection (GC/MS) are typically utilized to obtain isotopic data.[2−4] GC/MS is widely used because of the existence of established protocols for derivatizing metabolites and accessibility of compound libraries for the species fragmented upon electron impact ionization.[2,4−6] Recently, several investigations have utilized liquid chromatography coupled to mass spectrometry (LC−MS) for some applications in metabolic flux analysis.[7−11] Although LC−MS offers the advantage of analyzing many intracellular metabolites without derivatization, including phosphorylated compounds involved in glycolysis and the pentose phosphate pathway, the technique can be time-consuming, and reproducible separation is not always possible.

An alternative to these methods is the use of direct injection of the sample into the mass spectrometer. In order to detect with direct infusion all the species present in such a complex mixture, a high resolving power technique is needed. Fourier transform-ion cyclotron resonance mass spectrometry (FT-ICR MS) instruments achieve high resolution and, equipped with ESI sources, easily detect amino acids without derivatization. Furthermore, FT-ICR MS provides the capability to isolate individual species for MS/MS with high front-end resolution, allowing interrogation of structural isomers directly from complex mixtures. For these reasons, ESI FT-ICR MS is an ideal technology for profiling metabolites in a high-throughput fashion, without the need for a chromatographic separation. So far, few examples of direct

* Corresponding author. E-mail: keasling@berkeley.edu. Phone: 510-495-2620. Fax: 510-495-2630.

† Virtual Institute of Microbial Stress and Survival, Lawrence Berkeley National Laboratory.

‡ Physical Biosciences Division, Lawrence Berkeley National Laboratory.

§ Bruker Daltonics Inc.

∥ University of California.

(1) Stephanopoulos, G. N.; Aristidou, A. A.; Nielsen, J. *Metabolic Engineering: Principles and Methodologies*; Academic Press: San Diego, 1998.

(2) Szyperski, T. *Q. Rev. Biophys.* **1998**, *31*, 41−106.

(3) Peng, L.; Arauzo-Bravo, M.; Shimizu, K. *FEMS Microbiol. Lett.* **2004**, *235*, 17−23.

(4) Shimizu, K. *Adv. Biochem. Eng. Biotechnol.* **2004**, *91*, 1−49.

(5) Schauer, N.; Steinhauser, D.; Strelkov, S.; Schomburg, D.; Allison, G.; Moritz, T.; Lundgren, K.; Roessner-Tunali, U.; Forbes, M. G.; Willmitzer, L.; Fernie, A. R.; Kopka, J. *FEBS Lett.* **2005**, *579*, 1332−1337.

(6) Wiechert, W. *Metab. Eng.* **2001**, *3*, 195−206.

(7) Jander, G.; Norris, S. R.; Joshi, V.; Fraga, M.; Rugg, A.; Yu, S.; Li, L.; Last, R. L. *Plant J.* **2004**, *39*, 465−475.

(8) Matsuda, F.; Morino, K.; Ano, R.; Kuzawa, M.; Wakasa, K.; Miyagawa, H. *Plant Cell Physiol.* **2005**, *46*, 454−466.

(9) Oldiges, M.; Kunze, M.; Degenring, D.; Sprenger, G.; Takors, R. *Biotechnol. Prog.* **2004**, *20*, 1623−1633.

(10) Petersen, S.; Von Lieres, E.; De Graaf, A.; Sahm, H.; Wiechert, W. *Metab. Eng. Post Genomic Era* **2004**, 237−275.

(11) Boatright, J.; Negre, F.; Chen, X.; Kish, C. M.; Wood, B.; Peel, G.; Orlova, I.; Gang, D.; Rhodes, D.; Dudareva, N. *Plant Physiol.* **2004**, *135*, 1993−2011.

10.1021/ac061906b CCC: $37.00
Published on Web 02/17/2007

injection have been reported for target analysis of metabolites[12,13] and none for metabolic flux analysis.

To fully characterize the biochemical pathways of a living system using tracer experiments, along with the very useful information obtained from the abundances of the mass isotopomers, another crucial piece of information is the position of the labeled atom(s) in the skeleton of metabolites. In fact, different pathways could produce positional isotopomers and a simple mass spectrum would measure the same m/z value without differentiating the species.

The technique routinely utilized to determine the specific position of the labeled atom(s) in the backbone of the metabolite is NMR,[2] but several studies have reported success using GC/MS. Particularly interesting examples have shown determination of the ^{13}C atom position in glucose extracted from liver lysate.[14] In this case, fragmentation of glucose, derivatized with four different chemical agents, produced complementary patterns of product ions useful for determining the location of the labeled atom. Other interesting studies have aimed at elucidating biosynthetic routes[15] and determining the distribution of $^{13}C/^{12}C$ ratios at specific positions with high precision for organic compounds in complex mixtures.[16]

In this study, direct infusion into ESI FT-ICR MS was used to analyze the isotopomer distribution of amino acids in *Desulfovibrio vulgaris* Hildenborough, an environmentally important bacterium involved in global sulfur cycling and bioremediation.[17−19] This information could then be used in a metabolic model to calculate the fluxes through the central metabolic pathways that would be required to arrive at the experimentally determined, isotopomer distribution in the amino acids. In addition, FT-ICR MS was used to confirm the presence of specific enzymatic reactions for which there were no annotated genes: the position of the ^{13}C in the backbone of the two isotopomers $[^{13}C_1\text{-Glu} + H]^+$ and $[^{13}C_1\text{-Asp} + H]^+$ was used to confirm an unusual citrate synthase pathway in the tricarboxylic acid (TCA) cycle.[20,21] These two targeted amino acids were fragmented by SORI-CID.[22] The product ions generated upon CID retain labeled ^{13}C atoms in their backbone, allowing precise determination of their position.

Fragmentation reactions of the 20 α-amino acids have been systematically and extensively studied, both experimentally and theoretically.[23−42] Among those, a rigorous investigation of the product ions generated upon fragmentation of protonated phenylalanine and its derivatives[40] was performed. Similarly, fragmentation channels for protonated arginine and lysine,[41] as well as tyrosine,[42] have been characterized These studies have provided detailed reaction schemes for the acquired data, along with potential energy surface for competing fragmentation pathways, optimized three-dimensional structures with their relative energies, and in some cases unimolecular rate constants. The studies for all 20 α-amino acids have been summarized in a comprehensive review.[43]

This knowledge was utilized to determine precisely and unambiguously the position of the ^{13}C atom in the backbone of the two amino acids of interest. With this information available, unknown pathways activated under some physiological conditions can be unveiled and irreversible reaction steps can be investigated with a high degree of certainty.

MATERIALS AND METHODS

Bacterial Culture and Sample Preparation. *D. vulgaris* Hildenborough (ATCC 29579, Manassas, VA) were cultured in a modified defined LS4D sulfate medium[44] containing 99% [1-^{13}C]-L-lactate (Cambridge Isotope) at 30 °C in an anaerobic chamber (Coy Laboratory Products Inc, Grass Lake, MI) with an atmosphere of 5% CO_2, 5% H_2, and 90% N_2. A 50-mL culture in exponential phase ($OD_{600} = 0.4$) was harvested and centrifuged at 8000*g*. The cell pellets were washed once with 0.9% NaCl and flash frozen at −80 °C. The pellets were suspended in 1 mL of sterile Nanopure water and sonicated using the microtip for 3 min with a 3-s on/1-s off cycle and a power level of 30%. One milliliter of proteins lysate was precipitated by addition of 0.25 mL of 60

(12) Kruppa, G.; Schnier, P. D.; Tabei, K.; Van Orden, S.; Siegel, M. M. *Anal. Chem.* **2002**, *74*, 3877−3886.
(13) Aharoni, A.; Ric de Vos, C. H.; Verhoeven, H. A.; Maliepaard, C. A.; Kruppa, G.; Bino, R.; Goodenowe, D. B. *Omics* **2002**, *6*, 217−234.
(14) Beylot, M.; David, F.; Brunengraber, H. *Anal. Biochem.* **1993**, *212*, 532−536.
(15) Islam, N.; Bacala, R.; Moore, A.; Vanderwel, D. *Insect Biochem. Mol. Biol.* **1999**, *29*, 201−208.
(16) Corso, T. N.; Brenna, J. T. *Proc. Natl. Acad. Sci. U.S.A.* **1997**, *94*, 1049−1053.
(17) Ouattara, A.; Jacq, V. A. *FEMS Microbiol. Ecol.* **1992**, *101*, 217−228.
(18) Noguera, D. R.; Brusseau, G. A.; Rittmann, B. E.; Stahl, D. A. *Biotechnol. Bioeng.* **1998**, *59*, 732−746.
(19) Hadas, O.; Pinkas, R. *Microb. Ecol.* **1995**, *30*, 55−66.
(20) Gottschalk, G.; Barker, H. *Biochemistry* **1967**, *6*, 1027−1034.
(21) Gottschalk, G. *Eur. J. Biochem,* **1968**, *5*, 346−351.
(22) Gauthier, J.; Trautman, T.; Jacobson, D. *Anal. Chim. Acta* **1991**, *246*, 211−225.
(23) Balta, B.; Basma, M.; Aviyente, V.; Zhu, C.; Lifshitz, C. *Int. J. Mass Spectrom.* **2000**, *201*, 69−85.
(24) Bojesen, G. *J. Am. Chem. Soc.* **1987**, *109*, 5557−5558.
(25) Bouchonnet, S.; Hoppilliard, Y. *Org. Mass Spectrom.* **1992**, *27*, 71−76.
(26) Bouchonnet, S.; Gonnord, M.; Hoppilliard, Y.; Mauriac, C. *Biol. Mass Spectrom.* **1992**, *21*, 576−584.
(27) Bouchoux, G.; Bourcier, S.; Hoppilliard, Y.; Mauriac, C. *Org. Mass Spectrom.* **1993**, *28*, 1064−1072.
(28) Campbell, S.; Beauchamp, J. L.; Rempe, M.; Lichtenberger, D. L. *Int. J. Mass Spectrom. Ion Processes* **1992**, *117*, 83−99.
(29) Gorman, G. S.; Speir, J. P.; Turner, C. A.; Amster, I. J. *J. Am. Chem. Soc.* **1992**, *114*, 3986−3988.
(30) Jensen, F. *J. Am. Chem. Soc.* **1992**, *114*, 9533−9537.
(31) Locke, M. J.; McIver, R. T. *J. Am. Chem. Soc.* **1983**, *105*, 4226−4232.
(32) Meot-Ner, M.; Hunter, E. P.; Field, F. H. *J. Am. Chem. Soc.* **1977**, *99*, 5576−5583.
(33) O'Hair, R. A.; Reid, G. E. *Rapid Commun. Mass Spectrom.* **1998**, *12*, 999−1002.
(34) O'Hair, R. A.; Styles, M. L.; Reid, G. E. *J. Am. Soc. Mass Spectrom.* **1998**, *9*, 1275−1284.
(35) O'Hair, R. A.; Broughton, P. S.; Styles, M. L.; Frink, B. T.; Hadad, C. M. *J. Am. Soc. Mass Spectrom.* **2000**, *11*, 687−696.
(36) Somogyi, A.; Wysocki, V. H.; Mayer, I. *J. Am. Soc. Mass Spectrom.* **1994**, *5*, 704−717.
(37) Wu, J.; Lebrilla, C. B. *J. Am. Chem. Soc.* **1993**, *115*, 3270−3275.
(38) Zhang, K.; Zimmerman, D. M.; Chung-Phillips, A.; Cassady, C. J. *J. Am. Chem. Soc.* **1993**, *115*, 10812−10822.
(39) Kulik, W.; Heerma, W. *Biomed. Environ. Mass Spectrom.* **1988**, *17*, 173−180.
(40) Lioe, H.; O'Hair, R. A. *Org. Biomol. Chem.* **2005**, *3*, 3618−3628.
(41) Iris Shek, P. Y.; Zhao, J.; Ke, Y.; Siu, M.; Hopkinson, A. *J. Phys. Chem. A* **2006**, *110*, 8282−8296.
(42) Zhao, J.; Shoeib, T.; Siu, M.; Hopkinson, A. *Int. J. Mass Spectrom.* **2006**, *255−256*, 265−278.
(43) Rogalewicz, F.; Hoppilliard, Y.; Ohanessian, G. *Int. J. Mass Spectrom.* **2000**, *195/196*.
(44) Mukhopadhyay, A.; He, Z.; Alm, E. J.; Arkin, A. P.; Baidoo, E. E.; Borglin, S. C.; Chen, W.; Hazen, T. C.; He, Q.; Holman, H. Y.; Huang, K.; Huang, R.; Joyner, D. C.; Katz, N.; Keller, M.; Oeller, P.; Redding, A.; Sun, J.; Wall, J.; Wei, J.; Yang, Z.; Yen, H. C.; Zhou, J.; Keasling, J. D. *J. Bacteriol.* **2006**, *188*, 4068−4078.

wt % trichloroacetic acid. The protein pellet was washed with cold acetone two times and then hydrolyzed in 6 M HCl at 100 °C for 24 h. In the resulting amino acid mixture, cysteine and tryptophan were lost due to oxidation, and glutamine and asparagine were deaminated. For ESI FT-ICR MS analysis, the supernatant or the dried hydrolyzed sample was prepared in 1 mL of MeOH/H_2O (1/1) containing 1% formic acid. The resulting solution was amenable to ionization with an electrospray source.

ESI FT-ICR MS Conditions. The instrument used for these studies was a Bruker-Daltonics (Billerica, MA) Apex Qe Fourier transform ion cyclotron resonance mass spectrometer equipped with a Bruker-Magnex actively shielded superconducting magnet operating at 9.4 T and a Bruker-Daltonics Apollo I ESI source. A detailed description of this instrument and its performance has been published previously.[46] Samples were directly infused into the ESI source at a flow rate of 180 μL/h. The ESI source was operated in positive ion mode, with a nebulizing gas pressure of 40 psi, a drying gas temperature of 175 °C with source voltages of −4.5 kV on the atmospheric side of the glass capillary, −4.0 kV on the end cap shield of the glass capillary, and −2.0 kV on the cylinder shield. The value for the capillary exit voltage on the ESI source was set at 75 V. The ions produced were externally accumulated in a hexapole ion guide in the ESI source[46,47] for ∼2.0 s before being transferred to the FT-ICR MS cell, with a background pressure of $\sim 5 \times 10^{-11}$ mbar for detection. The operating software was XMASS version 7.8 (Bruker Daltonics).

CHEF and SORI-CID Conditions. The *c*orrelated *h*armonic *e*xcitation *f*ields (CHEF) technique was utilized to isolate the ion of interest in the FT-ICR MS analyzer cell, involving a specially calculated frequency swept rf excitation.[12] With CHEF isolation,[48] undesirable off-resonant excitation of the ion of interest was minimized by using a fixed duration for all the pulses in the sweep excitation and by slightly adjusting the frequency of each pulse so that the ion to be isolated was returned to its starting point at the end of the pulse. Calibration was performed externally using an amino acid standard mix (Sigma, St. Louis, MO), isolating the same amino acid on which MS^n in the real sample had to be performed. The concentration of the standard mix was 25 μM.

The conditions for MS^n CHEF isolation for this study were as follows. The pulse length used in the CHEF isolation was 200 μs, with an attenuation of 12 dB, which resulted in an excitation voltage of 75 V p−p on the transmitter plates. Fragmentations of the isolated analyte precursor ions were selectively activated by SORI-CID[22] in the following manner. Argon gas was pulsed into the ultrahigh-vacuum region containing the analyzer cell to a peak pressure of 1×10^{-6} mbar. A 4−8 V p−p rf pulse (30−40 dB attenuation), off-resonance from the precursor by 500 Hz, was applied for 200 ms. The voltage of the SORI-CID rf pulse was adjusted to give nearly complete attenuation of the precursor ion signal. Several seconds were allowed for fragmentation and for pumping away the collision gas, so that the fragments could be detected under high-resolution conditions at 1×10^{-10} mbar. In the time domain, 20−30 scans were acquired, consisting of 1024k data points each, signal averaged, apodized, and Fourier transformed (magnitude mode).

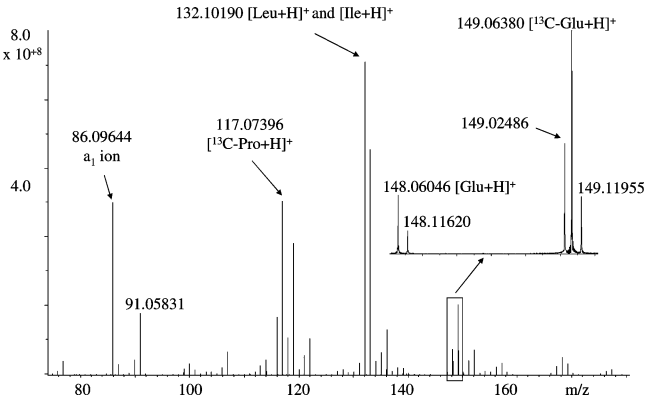

Figure 1. Positive-ion mode ESI FT-ICR MS of *D. vulgaris* hydrolysate. Expanded region shown in the inset.

GC/MS Conditions. GC/MS samples were prepared in 100 μL of tetrahydrofuran and 100 μL of *N*-(*tert*-butyldimethylsilyl)-*N*-methyltrifluoroacetamide (Sigma-Aldrich). All samples were derivatized in a water bath at 65−80 °C for 1 h. The GC conditions followed published protocols.[49] Two types of positively charged amino acid species were clearly observed by GC/MS: unfragmented molecules [M − 57] and fragmented species that lost one carboxyl group [M − 159]. The two fragmented molecules [M − 57 and M − 159] were used to determine whether the carboxyl group was labeled. At the beginning of each experiment, the mass spectrometer (lens system, quadrupole prefilters and main rods, detector) was thoroughly tuned, and unlabeled amino acids were run first as standards to obtain the correct retention times from the GC and to provide useful mass information in order to correct for natural isotopic effects.

RESULTS AND DISCUSSION

Isotopomer Measurement Using FT-ICR MS and GC/MS. The *D. vulgaris* lysate was directly infused into the FT-ICR MS (Figure 1). The hydrolyzed products were distributed in the range from m/z 70 to roughly m/z 180. The most prominent was the m/z 132.101 90 peak. From exact mass analysis, this peak corresponds to the molecular mass of protonated leucine (and isoleucine), with an error equal to 0.06 ppm (Table 1). This peak represents these two components in the mixture, as it is not possible to distinguish structural isomers using direct injection of the hydrolyzed sample, which is a limitation of the methodology.

Inspection of the MS of the *D. vulgaris* lysate unveiled the presence of interfering species very close to all the analytes of interest (Figure 1, inset), where the additional peaks surrounding $[Glu + H]^+$ and $[^{13}C\text{-}Glu + H]^+$ were distinctively detected. The high mass accuracy of the two isotopomers of glutamic acid (≤0.16 ppm), reported for convenience in Table 1, leads to their unambiguous identification. All the targeted protonated amino acid isotopomers detected, even the less abundant species (e.g., M3 Pro, M4 Leu, and M2 Tyr), had excellent signal/noise ratios (Table 1). Detection and relative quantification with FT-ICR MS of both highly abundant and less abundant components (<1%) is

(45) Tang, Y.; Pingitore, F.; Mukhopadhyay, A.; Phan, R.; Hazen, T.; Keasling, J. *J. Bacteriol.* **2007**, *189*, 940−949.
(46) Senko, M.; Hendrickson, C.; Emmett, M.; Shi, S.; Marshall, A. *J. Am. Soc. Mass Spectrom.* **1997**, *8*, 970−976.
(47) Wilcox, B. E.; Hendrickson, C. L.; Marshall, A. G. *J. Am. Soc. Mass Spectrom.* **2002**, *13*, 1304−1312.
(48) de Koning, L.; Nibbering, N.; van Orden, S.; Laukien, F. *Int. J. Mass Spectrom. Ion Processes* **1997**, *165/166*, 209−219.
(49) Dauner, M.; Sauer, U. *Biotechnol. Prog.* **2000**, *16*, 642−649.

Table 1. Relative Intensity and Error Associated with the Measurement of Each Amino Acid Isotopomer[a]

amino acid	rel intens (%)	error (ppm)	amino acid	rel intens (%)	error (ppm)	amino acid	rel intens (%)	error (ppm)	amino acid	rel intens (%)	error (ppm)
Gly			Val			Lys			Phe		
M0	1.30	0.21	M0	11.60	0.07	M0	0.90	0.15	M0	0.65	0.17
M1	4.20	0.22	M1	42.40	0.01	M1	4.20	0.09	M1	2.60	0.21
			M2	1.80	0.00	M2	8.00	0.10	M2	5.60	0.20
						M3	0.30	0.09	M3	3.70	0.21
Ala			Thr			Glu			Arg		
M0	4.70	0.00	M0	1.20	0.02	M0	8.30	0.16	M0	0.30	0.27
M1	19.50	0.01	M1	6.00	0.02	M1	23.30	0.08	M1	1.00	0.27
M2	0.40	0.00	M2	11.50	0.03	M2	1.00	0.09	M2	1.80	0.37
			M3	0.20	0.03				M3	0.07	0.21
Ser			Leu (and Ile)			Met			Tyr		
M0	2.30	0.03	M0	100	0.06	M0	0.15	0.17	M0	nd[b]	
M1	7.30	0.05	M1	71.70	0.01	M1	1.00	0.18	M1	0.10	0.25
M2	0.20	0.00	M2	4.20	0.01	M2	4.40	0.14	M2	0.20	0.42
			M3	0.10	0.04	M4	8.20	0.13	M3	0.15	0.15
Pro			Asp			His					
M0	19.00	0.03	M0	1.45	0.01	M0	2.40	0.12			
M1	55.20	0.02	M1	7.30	0.03	M1	3.80	0.12			
M2	2.50	0.02	M2	15.10	0.03	M2	0.90	0.09			
M3	0.06	0.40	M3	0.30	0.07	M4	0.30	0.08			

[a] M0, M1, M2, etc., refers to isotopomers with 0, 1, 2, etc., ^{13}C incorporated in the backbone of the amino acid. A RSD of ≤2% is associated with each relative inensity measurement. Errors refer to one single measurement. A variation of 10% is associated with it. [b] Not detected.

not surprising considering that a dynamic range of 10 000 has been reported.[50]

Due to the high concentration of amino acids (roughly estimated at ~10 μM) formed from acid hydrolysis of proteins, an absolute intensity on the order of 10^8 was easily obtained. While hydrolysis generated several other products (e.g., amines, fatty acids, etc.), these were not relevant for our investigation, and consequently, a search for their assignment was not performed.

One of the main objectives of this work was to profile the amino acid mass isotopomers obtained from *D. vulgaris*. To some extent, this approach is very similar to the use of FT-ICR MS for the relative quantification of peptides incorporating into their structure a stable isotope like O^{18} upon proteolytic cleavage.[51−53] GC/MS is the most widely used methodology to obtain isotopomer information. When analyzing amino acids by GC/MS, the amino acids must be derivatized to obtain volatile analytes. Besides being time-consuming, this process covalently binds other groups to the analyte, so that peak abundances of derivatized species do not actually reflect the abundance of the isotopomer distributions in the amino acid alone (due to the isotopomer contribution of the derivatizing agent incorporated in the backbone of the molecule). In this case, the isotope distribution of silicon (with natural abundances of 4.70 and 3.09% for ^{29}Si and ^{30}Si, respectively) in the derivatizing agent has a significant effect on the isotopomer distributions. Therefore, the raw data from GC/MS were corrected for isotopomer effects from the derivatizing groups, which is achieved by multiplying the isotopomer distribution vector of each derivatized amino acid by the corresponding correction matrices.[49] The corrected abundances of amino acids obtained from GC/MS measurements differed from those obtained with ESI FT-ICR MS by less than or equal to 2% of the relative standard deviation (Table 2). The sources of inaccuracy in GC/MS include incomplete resolution of adjacent ions, ion scattering, and peak tailing. Reliable isotopomer profiles for proline and arginine were not obtained by GC/MS but could be easily determined with ESI FT-ICR MS.

The direct infusion method has some disadvantages. Structural isomers like leucine and isoleucine cannot be differentiated, as already mentioned. However, for the analysis of fluxes in a known metabolic network, it is not necessary to determine the isotopomer patterns for all the amino acids (Figure 2); six key amino acids (His, Phe, Ser, Ala, Asp, Glu) are adequate to calculate the flux distributions through central metabolic pathways, including the TCA cycle and the pentose phosphate pathway. The remaining amino acids provide additional information for error estimation.

Identification of Carbon Position in Aspartic Acid and Glutamic Acid Using FT-ICR MS. The precise determination of the position of ^{13}C in the skeleton of the amino acid is crucial to assess the biochemical pathway from which the metabolite originated. This is usually performed with 2-D ^{13}C NMR. However, the detection limit for ^{13}C NMR is high and requires large amounts of biomass.[2,54] GC/MS may be a valid alternative, but chromatographic separation and derivatization are needed. Moreover, from fragmentation patterns, it is possible to infer the position of the ^{13}C only if the α-carboxyl group of amino acids is labeled.[49]

In our determination of the carbon transition route through the TCA cycle, we demonstrated that ESI FT-ICR MS is able to locate the ^{13}C position in protonated $^{13}C_1$-glutamic and $^{13}C_1$-aspartic acid and thereby provides direct evidence about the transition of carbons from oxaloacetate (precursor of aspartic acid) to oxoglutarate (precursor of glutamic acid) in the TCA cycle in *D. vulgaris*.

(50) Limbach, P.; Grosshans, P.; Marshall, A. *Anal. Chem.* **1993**, *65*, 135−140.
(51) Yao, X.; Freas, A.; Ramirez, J.; Demirev, P. A.; Fenselau, C. *Anal. Chem.* **2001**, *73*, 2836−2842.
(52) Everley, P. A.; Bakalarski, C. E.; Elias, J. E.; Waghorne, C. G.; Beausoleil, S. A.; Gerber, S. A.; Faherty, B. K.; Zetter, B. R.; Gygi, S. P. *J. Proteome Res.* **2006**, *5*, 1224−1231.
(53) Johnson, K. L.; Muddiman, D. C. *J. Am. Soc. Mass Spectrom.* **2004**, *15*, 437−445.
(54) Wittmann, C.; Heinzle, E. *Biotechnol. Bioeng.* **1999**, *62*, 739−750.

Table 2. Measured Mass Distribution by GC/MS and ESI FT-ICR MS for ^{13}C-Labeled Amino Acids from *D. vulgaris* Hydrolysates[a]

	M0	M1	M2	M3	comments
glycine	23 (20)	77 (80)			
alanine	19 (19)	79 (80)	2 (1)		
serine	24 (22)	74 (78)	2		no signal is detected for M2 with GC/MS (background noise)
proline	28	79	3	<1	not detected with GC/MS
valine	18 (20)	79 (77)	3 (3)		
threonine	6 (5)	29 (31)	64 (64)	1	no signal is detected for M3 with GC/MS (background noise)
leucine	55 (69)	42 (29)	3 (2)	<1	FT-ICR cannot distinguish leucine and isoleucine ions. The measured value is the addition of two species
isoleucine	(47)	(51)	(2)		
asparate	5 (5)	30 (30)	65 (65)		
lysine	10 (10)	26 (29)	62 (61)	2	GC peak is weak
glutamate	23 (21)	73 (73)	4 (6)		
methionine	5 (6)	31 (30)	62 (60)	2 (4)	peak tailing in GC/MS is observed
histidine	30 (30)	53 (53)	11 (9)	6 (8)	
phenylalanine	6 (6)	22 (21)	39 (39)	33 (34)	
arginine	10	33	55	2	GC could not detect clearly arginine
tyrosine		21 (18)	48 (50)	31 (32)	GC peak is weak

[a] ^{13}C-Labeled biomass was sampled in the middle log phase in the LS4D medium ($n = 2$). The standard errors for mass distributions between four replicates measurements by FT-ICR and GC/MS are less than 2% RSD.

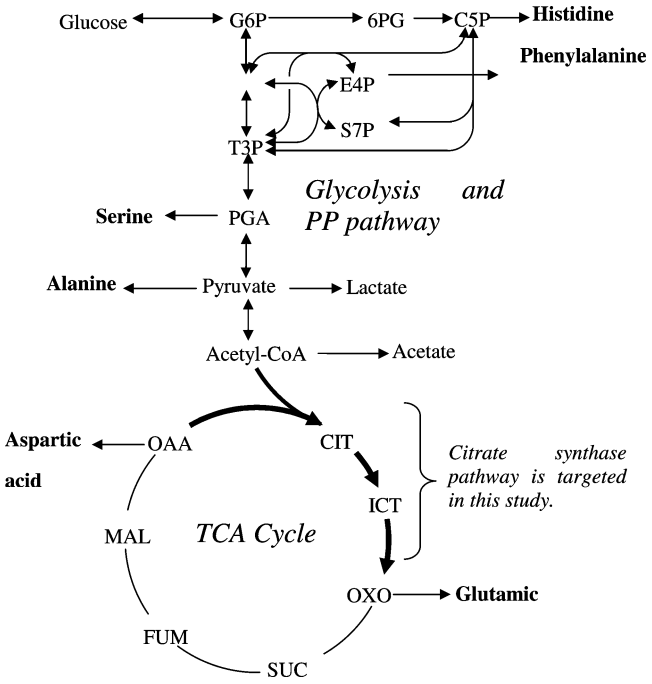

Figure 2. Central metabolic pathways in *D. vulgaris*. The six key amino acids from the central metabolic pathways necessary for flux analysis are shown in boldface type.

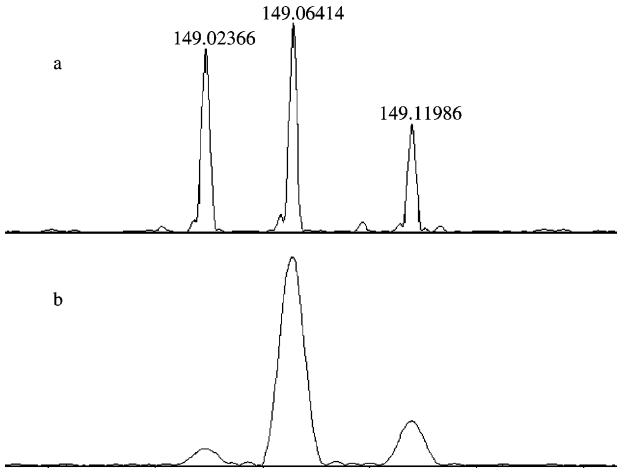

Figure 3. Isolation stages in the ICR cell of singly ^{13}C-labeled, protonated glutamic acid from *D. vulgaris* hydrolysate. (a) Expanded mass spectrum in the proximity of $[^{13}C_1\text{-Glu} + H]^+$ ion. (b) CHEF isolation of the $[^{13}C_1\text{-Glu} + H]^+$ species.

The technique CHEF was used to isolate $[^{13}C_1\text{-Glu} + H]^+$ with an m/z equal to 149.064 14. Before isolation, the species of interest was surrounded by two interfering peaks, only 0.04 and 0.06 Da apart (Figure 3a). When the CHEF frequency was applied, the desired ion became dominant (Figure 3b). This is clear evidence of the great versatility of this technique to isolate the ions of interest, even when the interfering species are extremely close, eliminating the need for any chromatographic separation, and therefore making the analysis faster. Subsequent to ion isolation, fragmentation of the selected molecular ion was induced by SORI-CID using a +500 Hz off-resonance excitation field. Fragmentation reactions of protonated glutamic acid have been studied extensively,[55−57] and many details about structures of its product ions and fragmentation patterns at different energy levels are known. The most prominent fragmentation reactions of protonated glutamic acids involve loss of H_2O, CO + H_2O, and CO + $2H_2O$, in some sequence. Some of the structures of the most relevant product ions generated upon CID are depicted in Scheme 1, as already proposed by Harrison and co-workers.[56,57] It has been established, in agreement with the known instability of α-amino-acylium ion,[58] that CO loss always occurs from the α-carboxylic

(55) Milne, G. W.; Axenrod, T.; Fales, H. M. *J. Am. Chem. Soc.* **1970**, *92*, 5170−5175.
(56) Dookeran, N.; Yalcin, T.; Harrison, A. *J. Mass Spectrom.* **1996**, *31*, 500−508.
(57) Harrison, A. G. *Int. J. Mass Spectrom.* **2001**, *210/211*, 361−370.
(58) Beranova, S.; Cai, J.; Wesdemiotis, C. *J. Am. Chem. Soc.* **1995**, *117*, 9492−9501.

Scheme 1. Dissociation Pathways of Protonated Glutamic Acid

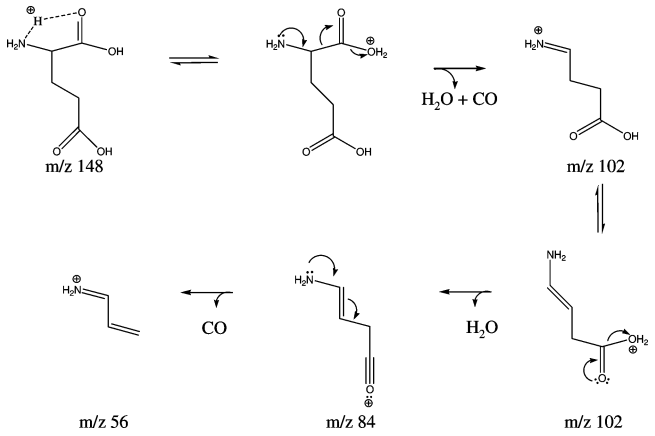

group in both CO + H_2O and CO + $2H_2O$ elimination regardless of the structure or the population of structures that may be involved in the different fragmentation channels. Moreover, formation of an ion with *m/z* 56 has been reported,[57] but details of its formation were not addressed in the study. However, this loss is easily explained as a fragmentation process involving CO elimination from the product ion at *m/z* 84. A possible fragmentation process leading to the formation of the acylium ion of 4-amino-3-butenoic acid (*m/z* 84), which undergoes a facile CO elimination (Scheme 1).[59,60] This proposed mechanism was further corroborated by our data, showing that this loss occurs from the γ-carboxylic group. The data from the experiments described here accurately matched existing data. SORI-CID is particularly well suited for the fragmentation process of amino acids, as low-energy rearrangement processes are highly favored.[22] Moreover, abundances of the product ions in the MS^2 spectrum of [^{13}C-Glu + H]$^+$ (Figure 4a and b) exactly matched abundances shown on the breakdown graphs[56,57] at high-energy regimes, generated with a cone voltage CID.[61,62] Such similar intensities at the high-energy levels indicates that large amounts of internal energy are deposited into the species of interest, and the fragmentation process occurs with high efficiency.[63,64]

The MS^2 SORI-CID spectrum (Figure 4a), as expected, was dominated by the fragments generated upon H_2O loss (*m/z* 131.053 14) and more prominently by loss of CO + $2H_2O$ (*m/z* 85.047 73). The fragment generated upon loss of H_2O + CO was less abundant (*m/z* 103.058 27, Figure 4a). As previously stated (see Scheme 1), the first CO loss occurs uniquely from the α-carboxylic group. In fact, the product ions at *m/z* 103.058 27 (loss of H_2O + CO) and at *m/z* 85.047 73 (loss of $2H_2O$ + CO) accurately matched the incorporation of one ^{13}C atom in the product ion skeleton. The small mass errors shown next to the molecular masses for the protonated glutamic acid gave additional confidence in the correctness of the predicted elemental formulas for the observed fragment ions and confirmed the proposed

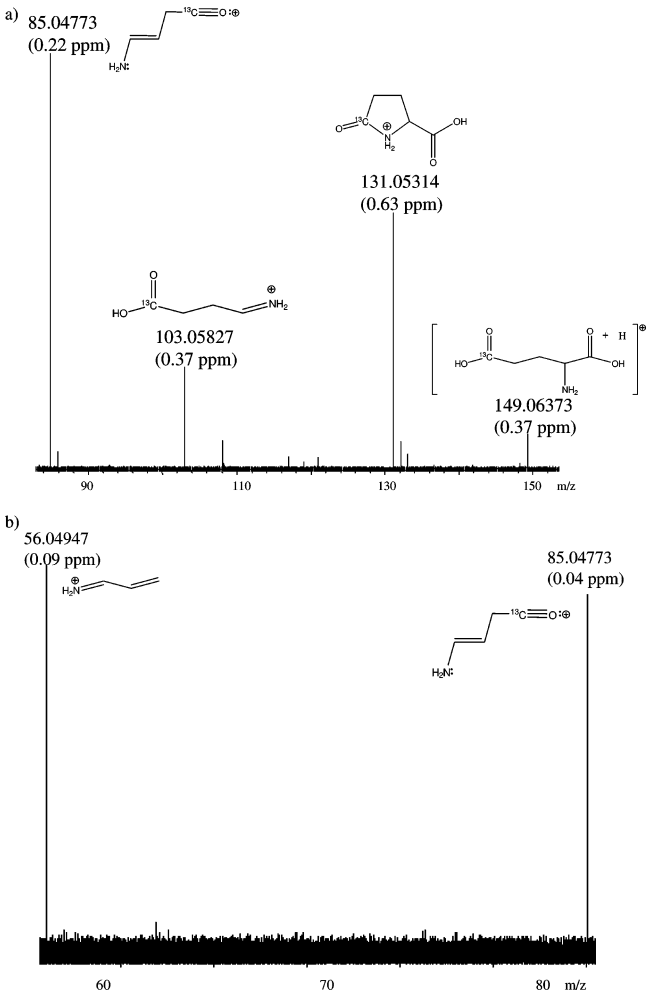

Figure 4. Multistage mass spectrometry experiments of singly ^{13}C-labeled, protonated glutamic acid from *D. vulgaris* hydrolysate. (a) SORI-CID (MS^2) of [$^{13}C_1$-Glu + H]$^+$. (b) SORI-CID (MS^3) of *m/z* 85.

structures in Harrison's studies.[56,57] Moreover, this fragmentation pattern was identical to the product ions generated in the ICR cell for a sample containing glutamic acid as a standard (data not shown).

The MS^2 SORI-CID experiment (Figure 4a) ruled out the presence of a ^{13}C atom in the α-position, but did not locate it in the amino acid backbone. For this reason, another MS stage was performed, and the ion *m/z* 85.047 73 was selected as the precursor. The resulting MS^3 experiment (Figure 4b) gave a very clean spectrum with the sole and sharp loss of ^{13}CO from the acylium ion of 4-amino-3-butenoic acid in accordance with Scheme 1. These data unequivocally establish the position of the ^{13}C atom in the γ-position showing furthermore the great versatility of the CHEF technique and SORI-CID as a valuable tool to isolate and fragment an amino acid of interest. The same methodology was utilized to determine the position of the labeled carbon in protonated $^{13}C_1$-aspartic acid. In the expanded region of the FT-ICR MS spectrum of [^{13}C-Asp + H]$^+$ (Figure 5a), the interfering peak was just 0.01 Da apart and even more abundant than the species of interest. Impressively, upon isolation, the interfering species was minimized (Figure 5b). Subsequent fragmentation generated the expected product ions[56,65] (Table 3), consistent with the mechanism proposed by Harrison (Scheme 2).

(59) Cordero, M. M.; Houser, J. J.; Wesdemiotis, C. *Anal. Chem.* **1993**, *65*, 1594−1601.
(60) Tsang, C.; Harrison, A. *J. Am. Chem. Soc.* **1976**, *98*, 1301−1308.
(61) Loo, J. A.; Udseth, H. R.; Smith, R. D. *Rapid Commun. Mass Spectrom.* **1988**, *2*, 207−210.
(62) Harrison, A. G. *Rapid Commun. Mass Spectrom.* **1999**, *13*, 1663−1670.
(63) Sleno, L.; Volmer, D. A. *J. Mass Spectrom.* **2004**, *39*, 1091−1112.
(64) Mcluckey, S. A.; Goeringer, D. E. *J. Mass Spectrom.* **1997**, *32*, 461−474.

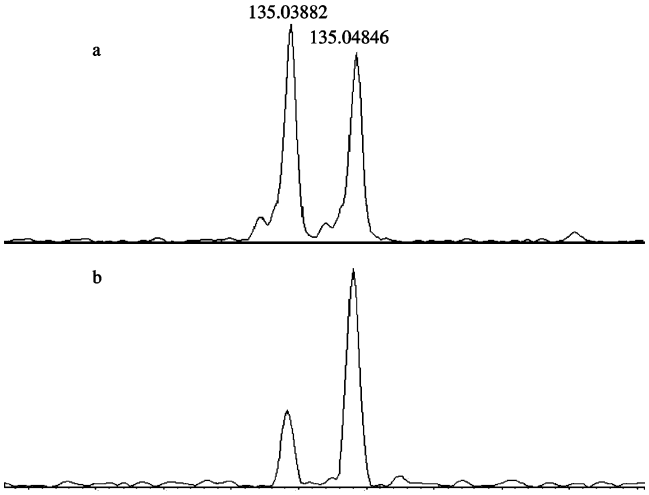

Figure 5. Isolation stages in the ICR cell of singly ^{13}C-labeled, protonated aspartic acid from *D. vulgaris* hydrolysate. (a) Expanded mass spectrum in proximity of $[^{13}C_1\text{-Asp} + H]^+$ species. (b) CHEF isolation of the $[^{13}C_1\text{-Asp} + H]^+$ species.

Table 3. SORI-CAD (MS^2) Spectrum of $[^{13}C\text{-Aps} + H]^+$ Generated by Positive Ion Mode ESI

Ion structures (abundance of $^{13}C/^{12}C$)	Neutral Loss	Measured m/z	Theoretical m/z	Error (ppm)
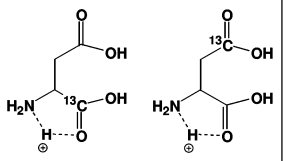 $[^{13}C\ Asp + H]^+$		135.048058	135.048139	0.60
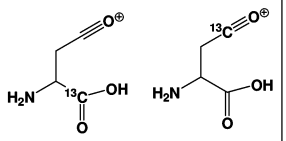	H_2O	117.037569	117.037574	0.05
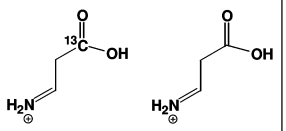	$H_2O + CO$	89.042664	89.042660	0.04
	$H_2O + {}^{13}CO$	88.039308	88.039305	0.03
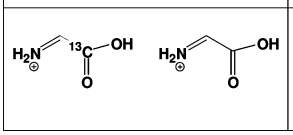	CH_2CO	75.027003	75.027010	0.10
	$CH_2{}^{13}CO$	74.023641	74.023655	0.19

The fragmentation process unveiled the presence of two mass isotopomers, namely, [1-^{13}C]- and [4-^{13}C]aspartic acid. However, mass spectrometrical measurements for the localization of ^{13}C in the aspartic backbone did not conclusively prove that the labeled atom was in the fourth position. In fact, the neutral loss was a ketene molecule, and the one labeled atom may have been present on both carbons, still giving rise to the same m/z value. However, based on the proposed carbon transition pathway in the TCA cycle (Figure 6), the C3 position in oxaloacetate (precursor of aspartic acid) corresponds to the C2 in oxoglutarate (precursor of glutamic acid). The MS^3 experiments on $[^{13}C_1\text{-Glu} + H]^+$ ruled out the presence of any ^{13}C in that position; therefore, all evidence indicates the presence of two mass isotopomer populations labeled at the first and fourth positions of the aspartic acid backbone. Furthermore, analysis of fragmentation patterns of $[^{13}C_2$ Asp + $H]^+$ (data not shown) clearly established that the two ^{13}C atoms resides at the α- and β-carboxylic group positions, showing the versatility of this methodology for analysis of different isotopomers of the same amino acid.

In summary, the FT-ICR MS methodology clarifies the carbon transition routes from oxaloacetate to oxoglutarate (Figure 6): fifth carbon (#) in oxoglutarate originated from the fourth carbon of oxaloacetate; the first carbon (∗) from oxaloacetate is lost as CO_2;

Scheme 2. Dissociation Pathways of Protonated Aspartic Acid

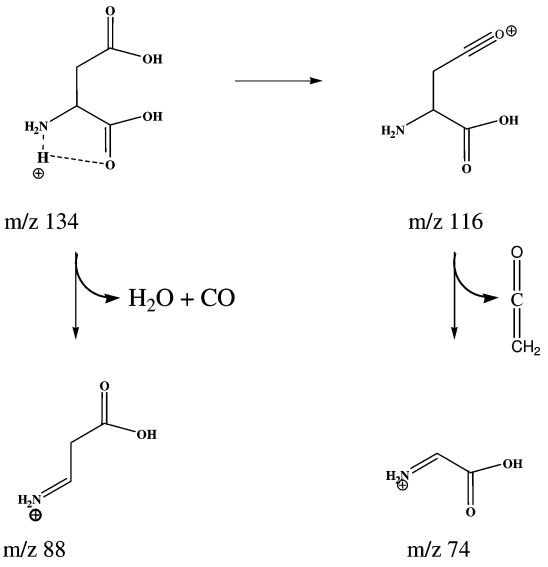

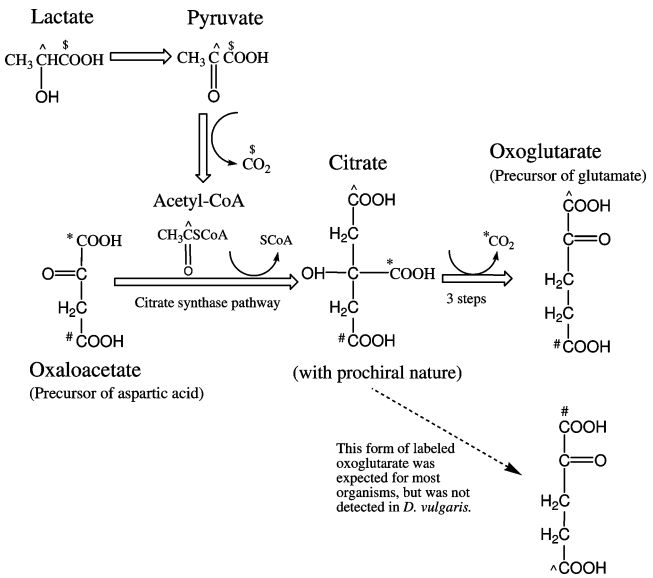

Figure 6. Carbon transition routes from oxaloacetate (indicated by aspartic acid) to oxoglutarate (indicated by glutamic acid).

(65) Harrison, A.; Tu, Y. *J. Mass Spectrom.* **1998**, *33*, 532−542.

the first carbon in oxoglutarate (^) originated from carbon of acetyl-CoA. This observation confirmed that citrate has a prochiral nature in the TCA cycle. The biological significance of this special pathway has been discussed elsewhere.[45] This study demonstrates the application of the FT-ICR MS technique to investigate unusual pathways in vivo and to utilize both the high-resolution and high front-end resolution MS/MS of FT-ICR MS to provide rich information for isotopomer analysis in a particular biological system. The methodology outlined in this investigation is applicable to any microorganisms to profile their amino acid isotopomer distributions. Moreover, as the α-amino acid fragmentation channels for the major reactions have been catalogued,[43] this information may enable researchers to precisely and unambiguously determine position(s) of any labeled atom(s) for every amino acid.

ACKNOWLEDGMENT

We thank Julie Leary and Chris Petzold for helpful suggestions and comments, Edward Baidoo and Peter Benke for analytical assistance, and Terry C. Hazen and Aindrila Mukhopadhyay for advice about bacteria growth. This work is part of the Virtual Institute for Microbial Stress and Survival (http://vimss.lbl.gov) supported by the U.S. Department of Energy, Office of Science, Office of Biological and Environmental Research, Genomics:GTL Program through contract DE-AC02-05CH11231 between the Lawrence Berkeley National Laboratory and the U.S. Department of Energy. F.P. and Y.T. contributed equally in this study.

Received for review October 9, 2006. Accepted January 24, 2007.

AC061906B